# Mobility Enhancement in Thin Silicon Films: Strain and Thickness Dependences of the Effective Masses and Non-Parabolicity Parameter

Viktor Sverdlov, Thomas Windbacher, and Siegfried Selberherr
Institute for Microelectronics, TU Wien
Gußhausstraße 27-29/E360
A-1040 Wien, Austria
{sverdlov|windbacher|selberherr}@iue.tuwien.ac.at

*Abstract*— **A two-band k·p model is used to describe the subband structure in strained thin silicon films. The model provides the dependence of the conductivity effective mass on both strain and film thickness simultaneously. The shear strain induced decrease of the conductivity effective mass is more pronounced in stressed thin silicon films. This conductivity mass decrease ensures the mobility enhancement in MOSFETs even with extremely thin silicon films. The two-band k·p model also describes the non-parabolicity dependence on film thickness and on strain. The dependence of the non-parabolicity parameter on both film thickness and strain reduces the mobility enhancement due to the conductivity mass modification in advanced MOSFETs with strained ultra-thin silicon body.**

***Keywords - two-band k·p model, subband structure, shear strain, effective masses, nonparabolicity, Monte Carlo methods***

## I. INTRODUCTION

An amazing size reduction of semiconductor devices supports the rapid increase in computational power and speed of integrated circuits. With scaling apparently approaching its fundamental limits, the semiconductor industry is facing an increasing number of critical challenges. New engineering solutions and innovative techniques are required to further improve CMOS device performance. Successful downscaling of MOSFETs can now be possible only when innovative changes and new materials are introduced in the technological processes. The 45 nm MOSFET process technology recently developed by Intel [1] introduces new hafnium-based high-k dielectric materials and metal gate, representing a major change in the technological process since the invention of MOSFETs. However, previously employed strain-induced mobility enhancement technology remains the most attractive solution to increase the device speed and will certainly take a key position among other technological changes for the next technology generations. Although alternative channel materials with a mobility higher than in Si are actively investigated [2, 3], it is believed that strained Si will be the main channel material for MOSFETs down to the 22 nm technology node [3].

A multi-gate MOSFET architecture is expected to be introduced for the 22 nm technology node. Combined with a high-k dielectric/metal gate technology and strain engineering, a multi-gate MOSFET appears to be the ultimate device for high-speed operation with excellent channel control, reduced leakage currents, and low power budget. Confining carriers within thin Si films reduces the channel dimension in transversal direction, which further improves gate channel control. The quantization energy in ultra-thin Si films may reach several hundred meV. The parabolic band approximation usually employed for subband structure calculations of confined electrons in Si inversion layers will likely be insufficient in ultra-thin Si films. A recent study of subband energies and transport in (001) and (110) oriented thin Si films reveals that even the non-parabolic isotropic dispersion is not sufficient to describe experimental data, and a direction-dependent anisotropic non-parabolicity must be introduced [4].

A comprehensive analysis of transport in multi-gate MOSFETs under general stress conditions is therefore required in order to understand the enhancement of device performance. Besides the biaxial stress obtained by epitaxially growing Si on a SiGe substrate, modern stress engineering techniques allow the generation of large uniaxial stress along the [110] channel. Stress in the [110] direction induces significant shear lattice distortion. The influence of the shear distortion on the subband structure and low-field mobility has not yet been carefully analyzed.

The two-band **k·p** model [5-8] provides a general framework to compute the subband structure, in particular the dependence of the electron effective masses on shear strain. In case of a square potential well with infinite walls, which is a good approximation for the confining potential in ultra-thin Si films, the subband structure can be obtained analytically [9], when inter-valley coupling is neglected. This allows an analysis of subband energies, effective masses, non-parabolicity, and the low-field mobility on film thickness for arbitrary stress conditions.

In the following we briefly review the main ideas behind the two-band **k·p** model for a valley in the conduction band of Si. Then we will shortly analyze the unprimed subband structure in (001) ultra-thin Si films, obtaining analytical dependences for the effective masses and the non-parabolicity parameter. With these parameters the non-parabolic subband

approximation for the subband dispersions will be constructed. The non-parabolic subband dispersions will be embedded into the subband Monte Carlo code in order to enable the computation of the low-filed mobility. Results of the mobility enhancement calculations will finally be analyzed.

## II. Conduction Band of Strained Silicon

From symmetry consideration it follows that the two-band **k·p** Hamiltonian of a [001] valley in the vicinity of the $X$ point of the Brillouin zone in Si must be of the form [6]:

$$H = \left( \frac{\hbar^2 k_z^2}{2m_l} + \frac{\hbar^2 (k_x^2 + k_y^z)}{2m_t} \right) I + \left( D\varepsilon_{xy} - \frac{\hbar^2 k_x k_y}{M} \right) \sigma_z + \frac{\hbar^2 k_z k_0}{m_l} \sigma_y \quad ,(1)$$

where $\sigma_{y,z}$ are the Pauli matrices, $I$ is the 2x2 unity matrix, $m_t$ and $m_l$ are the transversal and the longitudinal effective masses, $k_0 = 0.15 \times 2\pi / a$ is the position of the valley minimum relative to the $X$ point in unstrained Si, $\varepsilon_{xy}$ denotes the shear strain component, $M^{-1} = m_t^{-1} - m_0$, and $D$=14 eV is the shear strain deformation potential [5-8]. The two-band Hamiltonian results in the following dispersions [6]:

$$E = \frac{\hbar^2 k_z^2}{2m_l} + \frac{\hbar^2 (k_x^2 + k_y^2)}{2m_t} \pm \sqrt{\left( \frac{\hbar^2 k_z k_0}{m_l} \right)^2 + \delta^2} , \quad (2)$$

were the negative sign corresponds to the lowest conduction band,

$$\delta^2 = (D\varepsilon_{xy} - \hbar^2 k_x k_y / M)^2 . \quad (3)$$

We stress that all the moments as well as energies in (2) are counted from the $X$-point of the Brillouin zone. The accuracy of (2) was checked against the empirical pseudo-potential band structure calculations with parameters from [7,10] and excellent agreement was found up to 0.5 eV energy.

## III. Subband Effective Masses

The subband energies can be found analytically for an infinite square well potential which is a good approximation for an ultra-thin Si film. The analytical dispersion relation for the unprimed subbands in a [001] thin Si film of thickness $t$ can be found by neglecting weak inter-valley coupling [9]:

$$E_n(k_x, k_y) = E_n^0(k_x, k_y) - \delta^2 m_l / [2\hbar^2 k_0^2 (1 - q_n^2)], \quad (4)$$

where $q_n = (\pi n)/(t k_0)$ and $E_n^0$ is the subband dispersion for parabolic bands:

$$E_n^0(k_x, k_y) = \frac{\hbar^2 \pi^2 n^2}{2m_l t^2} + \frac{\hbar^2 (k_x^2 + k_y^2)}{2m_t} - \frac{\hbar^2 k_0^2}{2m_l} . \quad (5)$$

(4) is valid when

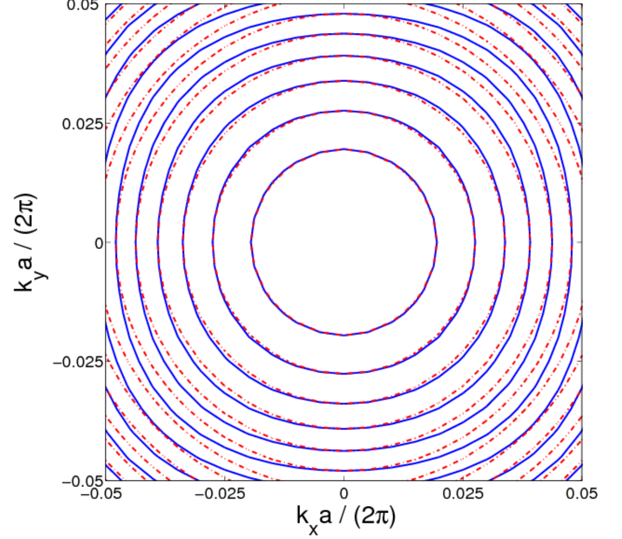


Figure 1. Subband dispersion (4) (solid) as compared to the parabolic approximation (dotted), for an unstrained film of thickness $t$=5.4 nm. The spacing between lines is 10 meV.

$$\left(1 - q_n^2\right)^2 > \delta^2 m_l^2 / \hbar^4 k_0^4 . \quad (6)$$

Dispersion (4) of the lowest subband in an unstrained thin film is compared to the parabolic approximation (5) in Fig.1. Non-parabolicity due to the last term in (4) becomes pronounced at an energy of 50 meV. We discuss the non-parabolicity parameter in the next section.

(4) also describes the subband dispersion in strained films. The quantization energy correction due to shear strain with respect to the valley minimum is:

$$\Delta E_n(\varepsilon_{xy}) = -\frac{\pi^2 n^2}{2m_l t^2} \frac{(D\varepsilon_{xy} m_l)^2}{\hbar^2 k_0^4 (1 - q_n^2)} . \quad (7)$$

(7) is obtained after taking into account the strain-induced valley minimum energy shift $\Delta E(\varepsilon_{xy}) = -(D\varepsilon_{xy})^2 m_l / (2\hbar^2 k_0^2)$ and the dependence of the longitudinal mass $m_l$ on strain [7, 8]:

$$m_l(\varepsilon_{xy}) = m_l \left(1 - (D\varepsilon_{xy} m_l)^2 / \hbar^4 k_0^4\right)^{-1} .$$

(4) also describes corrections to the transversal mass $m_t$ due to strain $\varepsilon_{xy}$, thickness $t$, and subband number $n$:

$$m_t^{\mp} = m_t \left( 1 \pm \frac{D\varepsilon_{xy} m_l}{\hbar^2 k_0^2} \frac{m_t}{M} \frac{1}{1 - q_n^2} \right)^{-1} \quad (8)$$

Here $m_t^-$ is the effective mass along the direction [110] of tensile stress. In thin films the effective mass depends not only on strain but also on film thickness. (8) is compared to the corresponding dependence in bulk silicon in Fig.2. The thickness dependence of the last term in (8) leads to a more pronounced anisotropy in the transversal mass than in a bulk semiconductor.

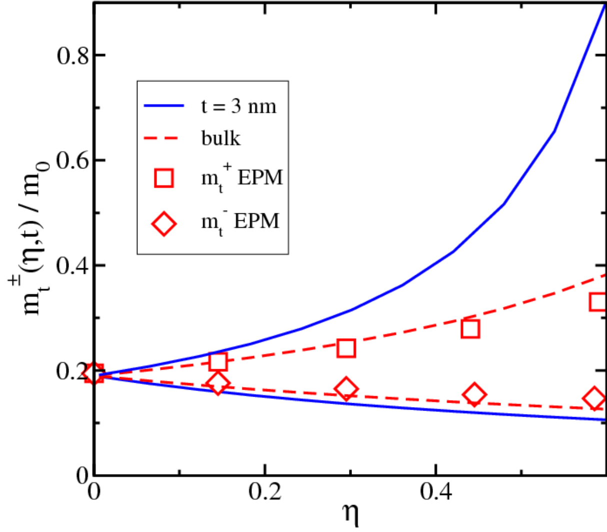


Figure 2. Strain-modified subband effective mass (solid lines). The strain dependence of the transversal mass in bulk silicon is shown by dashed lines and symbols (results of pseudo-potential calculations).

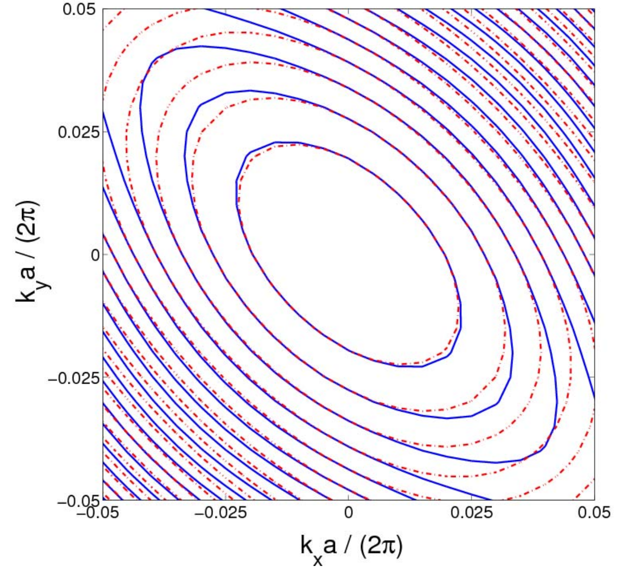


Figure 3. Subband dispersion (4) (solid) as compared to the parabolic approximation (dotted), for a film of thickness t=5.4 nm with 1 % of shear strained. The spacing between lines is 10 meV.

A comparison of the dispersion relation (4) to the parabolic approximation with transversal masses (8) for a strained film ( $\varepsilon_{xy} = 1\%$ ) of thickness $t$=5.4 nm is shown in Fig.3 Deviations from the parabolic approximation become large for electron energies above 20 meV. Therefore, to compute the carrier concentration and mobility in thin Si films the subband non-parabolicity must be taken into account.

## IV. The Subband Non-Parabolicity

After taking into account the energy shift (7) and the subband effective mass modifications (8) the subband dispersion (4) close to the minimum is written as:

$$E_n(k_x,k_y) = \frac{\hbar^2\pi^2 n^2}{2m_l(\eta)t^2} - \frac{\hbar^2 k_0^2}{2m_l} - \Delta E(\eta) - \Delta E_n(\eta) + \frac{\hbar^2 k_-^{-2}}{2m_t^-(\eta)} + \frac{\hbar^2 k_+^2}{2m_t^+(\eta)} - \frac{\hbar^2 (k_-^2 - k_+^2)^2 m_l}{8M^2 k_0^2 (1-q_n^2)}, \tag{9}$$

where $k_\pm = (k_x \mp k_y)/\sqrt{2}$ and $\eta = Dm_l\varepsilon_{xy}/(\hbar k_0)^2$ . The last term in (9) is proportional to the fourth power of the momentum and describes the subband non-parabolicity. We evaluate the dependence of the non-parabolicity parameter $\alpha(\eta,t)$ on strain $\eta$ and film thickness $t$ by equating the density-of-states obtained from (9) and from the phenomenological expression

$$\frac{\hbar^2 k_-^{-2}}{2m_t^-(\eta)} + \frac{\hbar^2 k_+^2}{2m_t^+(\eta)} = E(1+\alpha(\eta,t)E).$$

the following expression for the non-parabolicity parameter ratio is obtained:

$$\alpha(\eta,t) = \alpha_0 \frac{1}{1-q_n^2} \frac{1+2\left(\frac{m_t}{M}\frac{1}{1-q_n^2}\eta\right)^2}{1-\left(\frac{m_t}{M}\frac{1}{1-q_n^2}\eta\right)^2}. \tag{12}$$

The non-parabolicity parameter depends on the film thickness $t$ via $q_n$ and strain $\eta$. We use (7) and (12) in order to evaluate the low-field mobility in FETs with ultra-thin Si films.

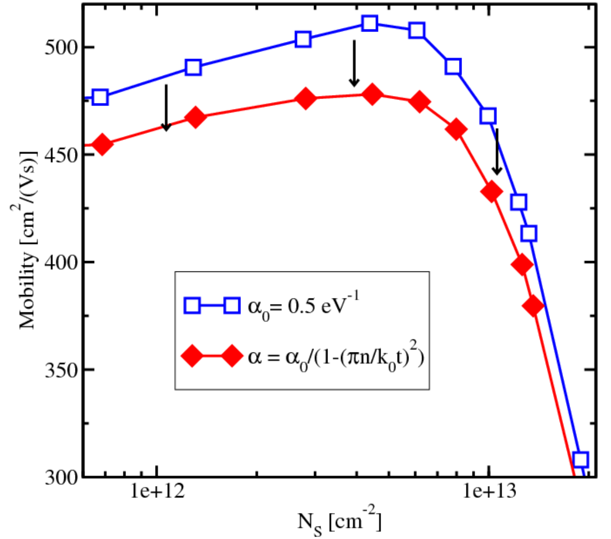


Figure 4. Mobility in a MOSFET with 3 nm unstrained UTB film. Due to thickness-dependent subband non-parabolicity the mobility slightly decreases.

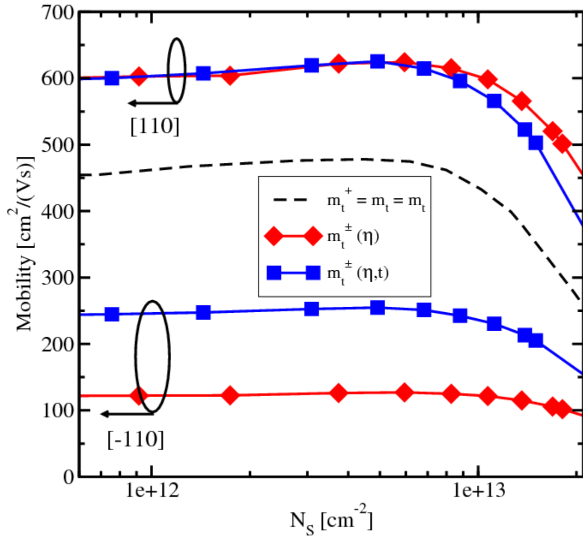


Figure 5. Mobility in a 3 nm unstrained (dashed line) and with 0.5% strain (diamonds) UTB FET. The squares are obtained with bulk values of the effective masses and the non-parabolicity parameter.

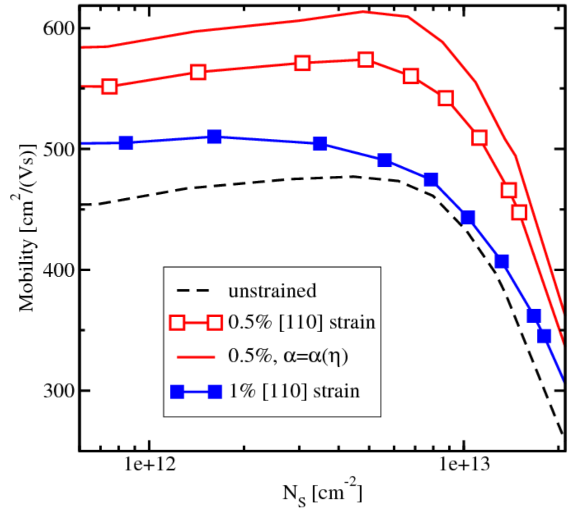


Figure 6. Influence of strain-dependent non-parabolicity on mobility. The dashed line denotes strain-independent non-parabolicity, open and filled symbols are for 0.5% and 1% strain, respectively.

A multi-subband Monte Carlo method designed for small signal analysis [11] was used to evaluate the mobility in MOSFETs with a thin Si film. The method is based on the solution of the linearized multi-subband Boltzmann equation and is exact in the limit of vanishing driving fields. The multi-subband method requires the subband wave functions and subband energies, which are calculated by solving the Schrödinger and the Poisson equations self-consistently. The wave functions are used to evaluate scattering rates with phonons and surface roughness. We calibrate the parameters of the Gaussian surface roughness correlation function by reproducing the universal mobility curve in the inversion layer. The same parameters are then used for mobility calculations in thin film MOSFETs. The surface roughness at the two thin film interfaces is assumed to be equal and uncorrelated.

An increase of $\alpha_n(t)$ leads to an increase of scattering, which results in a slight mobility decrease in a thin film even without stress as shown in Fig.4. Shear strain induces profound modifications in the subband dispersion. First, the dispersion becomes anisotropic, and the transversal mass develops two branches $m_t^+$ and $m_t^-$ shown in Fig.2. Due to the thickness-dependent factor $(1-q_n^2)^{-1}$ in (8), the strain-induced subband mass anisotropy is enhanced compared to the bulk. Surprisingly, an even smaller subband transport mass in tensile stress direction does not always result in a higher mobility enhancement as shown in Fig.5. The reason is the increase (10) of the subband non-parabolicity parameter with strain. This results in a higher density of states and increased scattering, with a stronger influence than the transport mass reduction at higher strain, which leads to the mobility enhancement decrease as shown in Fig.6.

## Acknowledgements

This work was supported in part by the Austrian Science Fund FWF, project P19997-N14.

## References

[1] K. Mistry, C. Allen, A.B. Beattie *et al.*, “A 45nm Logic Technology with High-k+Metal Gate Transistors, Strained Silicon, 9 Cu Interconnect Layers, 193nm Dry Patterning, and 100% Pb-free Packaging”, IEDM 2007, p.247.

[2] M.K. Hudati, G. Dewey, S. Datta, *et al.*, “Heterogeneous Integration of Enhancement Mode $In_{0.7}Ga_{0.3}As$ Quantum Well Transistor on Silicon Substrate using Thin (<2 um) Composite Buffer Architecture for High-Speed and Low-Voltage (0.5V) Logic Applications”, IEDM 2007, p.625.

[3] R. Chau, “Challenges and Opportunities of Emerging Nanotechnology for Future VLSI Nanoelectronics”, ISDRS 2007, ISBN: 978-1-4244-1892-3.

[4] K. Uchida, A. Kinoshita, M. Saitoh, “Carrier Transport in (110) nMOSFETs: Subband Structures, Non-Parabolicity, Mobility Characteristics, and Uniaxial Stress Engineering”, IEDM 2006, p.1019.

[5] J.C. Hensel, H. Hasegawa, and M. Nakayama, “Cyclotron Resonance in Uniaxially Stressed Silicon. II. Nature of the Covalent Bond”, *Phys.Rev.* **138**, A225-A238 (1965).

[6] G.L. Bir , G.E. Pikus, Symmetry and Strain-Induced Effects in Semiconductors, J.Wiley & Sons, NY, 1974.

[7] E. Ungersboeck, S. Dhar, G. Karlowatz, *et al.*, “The Effect of General Strain on the Band Structure and Electron Mobility of Silicon”, *IEEE Transactions on Electron Devices* **54**, 2183, (2007).

[8] V. Sverdlov, E. Ungersböck, H. Kosina, S. Selberherr, “Effects of Shear Strain on the Conduction Band in Silicon: An Efficient Two-Band k.p Theory”, ESSDERC 2007, ISBN: 1-4244-1124-6; p.386.

[9] V. Sverdlov, G. Karlowatz, S. Dhar, *et al.*, “Two-Band k·p Model for the Conduction Band in Silicon: Impact of Strain and Confinement on Band Structure and Mobility”, ISDRS 2007, ISBN: 978-1-4244-1892-3.

[10] M. Rieger and P. Vogl, “Electronic-Band Parameters in Strained $Si_{1-x}Ge_x$ Alloys on $Si_{1-y}Ge_y$ Substrates”, *Phys.Rev.* B **48**, 14275-14287, (1993).

[11] V. Sverdlov, E. Ungersboeck, H. Kosina, S. Selberherr, “Volume Inversion Mobiliy in SOI MOSFETs for Different Thin Body Orientation”, *Solid State Electronics* **51**, 299-305 (2007).